

# UC Davis

## UC Davis Previously Published Works

### Title

Contribution of Ryugu-like material to Earths volatile inventory by Cu and Zn isotopic analysis.

### Permalink

<https://escholarship.org/uc/item/4680m2vs>

### Journal

Nature Astronomy, 7(2)

### Authors

Paquet, Marine  
Moynier, Frederic  
Yokoyama, Tetsuya  
[et al.](#)

### Publication Date

2022-12-12

### DOI

10.1038/s41550-022-01846-1

Peer reviewed

Published in final edited form as:

*Nat Astron.* ; 7(2): 182–189. doi:10.1038/s41550-022-01846-1.

## Contribution of Ryugu-like material to Earth's volatile inventory by Cu and Zn isotopic analysis

*A full list of authors and affiliations appears at the end of the article.*

### Abstract

Initial analyses showed that asteroid Ryugu's composition is close to CI (Ivuna-like) carbonaceous chondrites –the chemically most primitive meteorites, characterized by near-solar abundances for most elements. However, some isotopic signatures (e.g., Ti, Cr) overlap with other carbonaceous chondrite (CC) groups, so the details of the link between Ryugu and the CI chondrites are not fully clear yet. Here we show that Ryugu and CI chondrites have the same zinc and copper isotopic composition. As the various chondrite groups have very distinct Zn and Cu isotopic signatures, our results point at a common genetic heritage between Ryugu and CI chondrites, ruling out any affinity with other CC groups. Since Ryugu's pristine samples match the solar elemental composition for many elements, their Zn and Cu isotopic compositions likely represent the best estimates of the solar composition. Earth's mass-independent Zn isotopic composition is intermediate between Ryugu/CC and non-carbonaceous chondrites, suggesting a contribution of Ryugu-like material to Earth's budgets of Zn and other moderately volatile elements.

### Keywords

Ryugu; Hayabusa2; Zn isotopes; Cu isotopes; volatile elements; CI chondrites

### Introduction

Ivuna-type (CI) carbonaceous chondrites (CCs) have elemental abundances that are the closest to the composition of the solar photosphere (e.g., [1]) (the exceptions being H, C, N, O, Li and the noble gases). Thus, the CIs are key reference samples for investigating how early Solar System processes shaped the compositions of the planets and their building

---

Users may view, print, copy, and download text and data-mine the content in such documents, for the purposes of academic research, subject always to the full Conditions of use: <https://www.springernature.com/gp/open-research/policies/accepted-manuscript-terms>.

\*corresponding author: [paquet@ipgp.fr](mailto:paquet@ipgp.fr), [moynier@ipgp.fr](mailto:moynier@ipgp.fr).

#### Author Contributions

F.M., M.P. and T.Y. designed the project. H.Y. and T.Y. coordinated the isotopic analyses of the samples among members of the Hayabusa2-initial-analysis chemistry team. M.P. and T.Y. processed the samples and separated the Zn and Cu from the matrix. M.P. measured the Zn and Cu isotopic compositions. M.P. and F.M. wrote the first draft of the manuscript, with contributions from T.Y., W. D., Y. H., Y. A., J. A., C. M. O'D. A., S. A., Y. A., K. B., M. B., A. B., R. W. C., M. C., B.-G. C., N. D., A. M. D., T. D. R., W. F., R. F., I. G., M. K. H., Y. H., H. Hi., H. Ho., P. H., G. R. H., K. I., T. I., T. R. I., A. I., M. I., S. I., N. K., N. T. K., K. K., T. K., S. K., A. N. K., M.-C. L., Y. M., K. D. McK., M. M., K. M., I. N., K. N., D. N., A. N. N., L. N., M. O., A. P., C. P. L. P., L. Q., S. S. R., N. S., M. S., L. T., H. T., K. T., Y. T., T. U., S. W., M. W., R. J. W., K. Y., Q.-Z. Y., S. Y., E. D. Y., H. Y., A.-C. Z., T. N., H. N., T. N., R. O., K. S., H. Y., M. A., A. M., A. N., M. N., T. O., T. Y., K. Y., S. N., T. S., S. Tan., F. T., Y. T., S.-I. W., M. Y., S. Tac. and H. Y.

#### Competing Interests Statement

The authors declare no conflicts of interest.

blocks. The return of the Hayabusa2 spacecraft in December 2020, after two successful touchdown and sampling events on the Cb-type asteroid (162173) Ryugu<sup>2,3</sup>, offers the unprecedented opportunity to study volatile element fractionation processes using samples unaffected by terrestrial alteration, in particular water incorporation. Initial studies on bulk chemical and isotopic compositions revealed similarities between Ryugu and CIs<sup>4-7</sup>. However, Ryugu samples exhibit slightly higher  $^{17}\text{O}$  than the average from other CI samples, Orgueil and Ivuna, which is interpreted in terms of original heterogeneity between small samples, or contamination of the meteorites by terrestrial water incorporated into the structure of the alteration minerals (e.g., phyllosilicates, sulfates, iron oxides and hydroxides), not adsorbed to the surfaces<sup>5</sup>. Similarly, although Ti and Cr isotope compositions show that asteroid Ryugu formed in the CC reservoir, it was not possible to establish a clear genetic link to just one of the CC groups because the Cr and Ti isotopic compositions of Ryugu overlap not only with Ivuna-like (CI) but also with the Bencubbin-like (CB)<sup>5</sup>, Renazzo-like (CR)<sup>5</sup> and High-iron (CH) groups. However, the low volatile contents of these three groups of meteorites, as well as the metal-rich nature of the CB and CH chondrites, argue against any affinity with Ryugu<sup>5,6</sup>. Thus, because CI chondrites and Ryugu samples share the same Ti and Cr nucleosynthetic signatures, as well as similar mineralogical and elemental compositions<sup>5,6</sup>, it has been proposed that they formed contemporaneously from the same outer Solar System reservoir<sup>3,5-7</sup>.

Material akin to carbonaceous chondrites such as Ryugu and the parent body of the CIs could have delivered significant fractions of the moderately and highly volatile elements present in inner Solar System planets (e.g., 8-13). Because Ryugu samples have been handled carefully to avoid possible contamination, they are ideally suited to estimate the solar composition and assess the contribution of these outer Solar System objects to the inventory of volatile elements in the terrestrial planets. Highly volatile and moderately volatile elements are defined as elements with 50% condensation temperatures ( $T_c$ ) <665 K and 665–1135 K, respectively, under canonical nebular gas conditions at  $10^{-4}$  bar (e.g., 14). Zinc and Cu are ideal elements to investigate volatility-related processes, such as volatile element loss, during planetary accretion<sup>15</sup>, and are classified as moderately volatile elements (MVE) (with  $T_c$  of 726 K and 1037 K, respectively)<sup>14,16</sup>. Carbonaceous chondrite groups display distinct Zn and Cu isotopic mass fractionation effects (e.g., 17-21), defining a trend from CIs to CKs (CK = Karoonda-like), with the CIs being the most volatile-rich and isotopically heaviest (for both Zn and Cu) of the CC groups. We have measured the Zn and Cu isotopic compositions of Ryugu samples to (i) verify the link between Ryugu and CI chondrites for moderately volatile elements, and (ii) assess the contribution of Ryugu-like material to the inventory of moderately volatile elements in Earth.

## Results

The Zn and Cu isotope compositions for four Ryugu samples (see Methods section), together with six CC samples [Alais (CI), Allende A and B (CV), Murchison (CM), Orgueil (CI), Tagish Lake (C2-ungrouped) and Tarda (C2-ungrouped)], were determined following the same analytical protocol, and on the same samples as in [5] (Table 1). Most of these

CC samples have previously been characterized for their Zn and Cu isotopic composition<sup>17–19,21</sup>, except Tarda. The isotopic compositions are given as the permil deviations from the JMC-Lyon Zn and NIST SRM976 Cu standards:

$$\delta^X \text{Zn} = \left[ \frac{\left( \frac{{}^x\text{Zn}}{64\text{Zn}} \right)_{\text{Sample}}}{\left( \frac{{}^x\text{Zn}}{64\text{Zn}} \right)_{\text{JMC-Lyon}}} - 1 \right] \times 1000 \quad (1)$$

where  $x = 66, 67$  and  $68$ .

$$\delta^{65} \text{Cu} = \left[ \frac{\left( \frac{65\text{Cu}}{63\text{Cu}} \right)_{\text{Sample}}}{\left( \frac{65\text{Cu}}{63\text{Cu}} \right)_{\text{SRM976}}} - 1 \right] \times 1000 \quad (2)$$

During the course of this study, the two standards gave  $\delta^{66}\text{Zn}$  of  $0.00 \pm 0.005$  ‰ (2SE;  $n = 163$ ; JMC-Lyon) and  $\delta^{65}\text{Cu}$  of  $0.00 \pm 0.02$  ‰ (2SE;  $n = 54$ ; NIST SRM976). Zinc isotope measurements are also corrected for mass-dependent fractionation using the exponential law<sup>22</sup>, with the normalizing ratio of  ${}^{68}\text{Zn}/{}^{64}\text{Zn}$  of  $0.3856$ <sup>23</sup>. Zinc isotopic anomalies are quantified using the epsilon notation relative to the JMC Lyon standard, as follows:

$$\epsilon^{66} \text{Zn}_c = \left[ \frac{\left( \frac{66\text{Zn}}{64\text{Zn}} \right)_{\text{Sample}}}{\left( \frac{66\text{Zn}}{64\text{Zn}} \right)_{\text{JMC-Lyon}}} - 1 \right] \times 10^4 \quad (3)$$

where  $c$  is the normalizing ratio  ${}^{68}\text{Zn}/{}^{64}\text{Zn}$ .

The Ryugu samples span a very limited range of mass-dependent Zn isotopic compositions with  $\delta^{66}\text{Zn}$  from  $+0.41 \pm 0.06$  ‰ to  $+0.45 \pm 0.02$  ‰ (2SD), with an average value of  $+0.43 \pm 0.05$  ‰ (2SD,  $n = 48$ ) (Fig. 1a and Table 1). The  $\delta^{65}\text{Cu}$  values for Ryugu samples range from  $0.00 \pm 0.08$  ‰ to  $+0.09 \pm 0.05$  ‰, (average value of  $+0.04 \pm 0.11$  ‰,  $n = 8$ , 2SD) (Fig. 1b and Table 1). Zinc and Cu abundances also span limited ranges from  $338 \pm 4$  ppm to  $383 \pm 6$  ppm (average  $361 \pm 40$  ppm,  $n = 4$ , 2SD), and from  $133 \pm 2$  ppm to  $168 \pm 1$  ppm (average  $147 \pm 37$  ppm,  $n = 4$ , 2SD), respectively (Table 2). These values are higher than the abundances reported for any CI chondrite, consistent with other element abundances for Ryugu samples relative to CIs (Fig. 1, Table 2), although Ryugu samples have lower  $\text{H}_2\text{O}$  contents than CIs<sup>5</sup>. It is worth noting that the samples from both landing sites show identical  $\delta^{66}\text{Zn}$  values (Fig. 1a). In addition, the soluble organic matter (SOM) extractions of samples C0107 and A0106, which was done prior to purification of Zn and Cu, do not seem to have affected the Zn and Cu isotope compositions of the

Ryugu samples (see Methods section). All the CCs measured in this study have  $\delta^{66}\text{Zn}$  and  $\delta^{65}\text{Cu}$  values, as well as Zn and Cu abundances, that are consistent with previous studies (e.g., [17–21]), except for the Cu isotopic composition for Allende A, which is more similar to CO chondrites (Figs. 1b and 2). We note, however, that until now only one other measurement of Allende has been reported in the literature<sup>19</sup>, and so the difference could represent heterogeneity in the different analyzed fractions of Allende in this study and in [19]. Similar sample heterogeneities for Cu isotopic compositions have been reported for several fragments of Orgueil<sup>21</sup>. The Ryugu samples exhibit Zn and Cu isotopic compositions that are similar to the Alais and Orgueil samples analyzed in this study (Figs. 1 and 2). This is consistent with previous work on the bulk elemental, isotopic, and mineralogical properties of these samples, which reveal a genetic link between the Ryugu samples and CI chondrites, implying formation from the same outer Solar System reservoir<sup>4–6</sup>.

## Discussion

Earlier work has shown that bulk CC chondrites define negative correlations in plots of  $\delta^{66}\text{Zn}$  versus  $1/\text{Zn}$ <sup>17,18</sup> and  $\delta^{65}\text{Cu}$  versus  $1/\text{Cu}$ <sup>19</sup>. The variable degree of volatile element depletion among the different CC groups reflect mixing of chemically and isotopically distinct reservoirs during their accretion (e.g., 17–19,24,25). The CI chondrites, along with Ryugu, are the least volatile depleted and isotopically heaviest (for both Zn and Cu) of the CC groups, while the most volatile depleted chondrites, the CVs, are the isotopically lightest (this study; [17–21]) (Figs. 1 and 2). The CC trend is interpreted as the result of mixing of volatile-rich material enriched in heavy Zn and Cu isotopes and volatile-poor material enriched in light Zn and Cu isotopes (e.g., [17–19]). Similar correlations are observed for other moderately volatile elements in CCs, such as Te<sup>25</sup> and Rb<sup>26,27</sup> and their associated isotope compositions, which is interpreted as mixing between matrix (volatile-rich) and chondrules (volatile-poor) (e.g., [17–19,24,26]). Such mixing between distinct CC reservoirs is also observed in the relationships between  $\delta^{66}\text{Zn}$  and nucleosynthetic isotope anomalies, such as  $\epsilon^{54}\text{Cr}$  (parts per ten thousand mass-independent variations of the  $^{54}\text{Cr}/^{52}\text{Cr}$  ratio relative to a terrestrial standard) (Fig. 3) (e.g., [18]). Ryugu and the CIs have similar Cu and Zn mass-dependent isotopic compositions and differ markedly from the CBs and CHs (Figs. 1, 2 and 3). We can, therefore, exclude any genetic relationship to the CB or CH groups for the Ryugu samples. A shared nucleosynthetic heritage between Ryugu and CI chondrites has been established based on their identical Ti and Cr nucleosynthetic isotope anomalies<sup>5,6</sup>. Our Zn and Cu results show that this parentage extends to mass-dependent fractionation of moderately volatile elements, strengthening the link between CI chondrites and Ryugu (Figs. 1, 2 and 3). The near solar Zn and Cu relative abundances of the Ryugu samples, which are free of the potential ambiguities of terrestrial alteration, suggests that the Zn and Cu isotopic compositions measured for Ryugu and the CI chondrites most likely preserved the proto-Sun's composition<sup>1</sup> (Fig. 1c).

Our study also provides evidence for mass-independent Zn isotope variations ( $\epsilon^{66}\text{Zn}$ ) in Ryugu samples (Fig. 4 and Table 1). These Zn isotopic anomalies are consistent with previous observations<sup>28,29</sup>. While non-carbonaceous chondrites (NCs) display negative  $\epsilon^{66}\text{Zn}$  (ordinary chondrites:  $-0.21 \pm 0.04$  ‰, 2SE,  $n = 12$ , [28,29]; enstatite chondrites:  $-0.19 \pm 0.08$  ‰,  $n = 8$ , [28,29]), the Ryugu samples and all CCs exhibit identical positive

$\epsilon^{66}\text{Zn}$  within error ( $+0.33 \pm 0.04 \text{‰}$ , 2SE, with  $n = 7$  for Ryugu (Table 1) and  $+0.39 \pm 0.07 \text{‰}$ ,  $n = 7$  for CCs, respectively) with the value previously reported for CC of  $+0.28 \pm 0.04 \text{‰}$  (2SE,  $n = 11$ ) [28,29]. It is worth noting that the first replicate of sample C0108 (measured at 100 ppb Zn) has an  $\epsilon^{66}\text{Zn}$  of  $-0.21 \pm 0.17 \text{‰}$ , whereas the second C0108 replicate (measured at 250 ppb Zn) has an  $\epsilon^{66}\text{Zn}$  of  $+0.35 \pm 0.10 \text{‰}$  similar to all other Ryugu samples (see Methods section): the first replicate is thus considered an outlier as it was analyzed at the lower concentration of 100 ppb and was excluded from the mean value reported here. The reference geological material BHVO-2 and the Zn standard solution IRMM 3702 measured during the first and second sessions have  $\epsilon^{66}\text{Zn}$  ( $-0.07 \pm 0.15 \text{‰}$ , 2SE,  $n = 12$ ;  $+0.02 \pm 0.11 \text{‰}$ , 2SE,  $n = 7$ , respectively), consistent within error with estimates for bulk Earth ( $+0.015 \pm 0.075 \text{‰}$ , 2SE,  $n = 4$  [28] and  $-0.07 \pm 0.013 \text{‰}$ , 2SE,  $n = 3$  [29]). There are no known terrestrial processes which can mass-independently fractionate Zn isotopes. The positive  $\epsilon^{66}\text{Zn}$  values in the Ryugu samples, therefore, reinforce their genetic link with the CCs (Fig. 4). Thus, the difference between the CCs and NCs, originally identified O and Cr isotope compositions<sup>30</sup>, and later with Ti, Ni and Mo anomalies<sup>31–36</sup>, appears to also hold for Zn isotopes.

Because meteorites show a large variability of isotope anomalies<sup>37</sup> and planetary accretion is stochastic<sup>38–39</sup>, it is likely that Earth's composition does not reflect accretion from a single type of material, both in terms of isotopic and elemental compositions. Although enstatite chondrites are isotopically closest to the Earth<sup>40</sup>, their chemical signatures are extreme and deviate substantially from the bulk composition of Earth. Possible mixtures of primitive and thermally processed meteorites or their components (e.g., chondrules; [6, 41–43]) have been proposed to explain the chemical and isotope composition of the Earth<sup>32,37,44–48</sup>. In particular, the mass-independent isotopic composition of Zn of the Earth appears intermediate between CCs and NCs. Thus, our new data show that CC-like materials, potentially akin to Ryugu, have likely contributed to the delivery of Zn and more generally the volatile elements to the Earth. Thus, following the same approach as in [28,29], and using the average  $\epsilon^{66}\text{Zn} = +0.33 \pm 0.04 \text{‰}$  for Ryugu,  $+0.35 \pm 0.13 \text{‰}$  for CI [this study, 28, 29],  $-0.20 \pm 0.04 \text{‰}$  (2SE,  $n = 20$ ) for NC (ordinary, enstatite from [28,29]) and  $-0.02 \pm 0.04 \text{‰}$  for the BSE (2SE,  $n = 7$ , [28,29]), the mass fraction of Ryugu- or CI-derived Zn in the BSE is estimated 33.5% or 32.2%, respectively. Thus, we find that ~30% of the terrestrial Zn derives from outer Solar System material, while the NC reservoir contributes to ~70% to the terrestrial Zn. Then, to account for the Zn abundances of the accreting materials by Earth, we estimate the mass fractions of NC and Ryugu-like or CI-like bodies accreted by Earth using the Zn abundance of the BSE of  $53.5 \pm 2.7 \text{ ppm}$  [49], and the  $[\text{Zn}]_{\text{Ryugu}}$  of  $361 \pm 40 \text{ ppm}$  [this study] and  $[\text{Zn}]_{\text{CI}}$  of  $309 \pm 43.8 \text{ ppm}$  [this study, 17,18,21]. Thus, up to ~5% of Ryugu-like material (or ~6% of CI-like material) might be needed to account for Earth's Zn isotopic composition, consistent with estimations from previous studies on Zn isotopic anomalies<sup>28,29</sup> and representing a substantial contribution to the terrestrial budget of moderately volatile elements<sup>11,28,29</sup>.

## Methods

### Major and trace elements

Zinc and copper isotopic compositions were measured in four samples from the asteroid (162173) Ryugu [C0108, C0107, A0106-A0107 and A0106]. Fragments A0106-A0107 and A0106 are coming from the first touchdown site, and C0108 and C0107 from the second touchdown site<sup>4-6</sup>. Samples A0106-A0107 and C0108 were pristine samples, whereas A0106 and C0107 were treated for Soluble Organic Matter (SOM) extraction before chemical purification (see Supplementary Table 1). In addition, six CCs [Alais, Allende A, Allende B, Murchison, Orgueil, Tagish Lake and Tarda] were processed following the exact same protocol as the Ryugu samples and were analyzed as controls. For each sample, ~25 mg of powder of all the samples were dissolved at Tokyo Institute of Technology. Elemental abundances were determined using Inductively-Coupled-Plasma Mass-Spectrometry (ICP-MS): major and trace elements for A0106-A0107 and C0108 samples are from [5]. After chemical analysis, the same sample solutions were used to determine Zn and Cu isotopic compositions: Zn fractions were pre-separated, as well as 3% of the bulk rock dissolution for Cu purification which represent about 80-100 ng of Cu.

### Zinc and copper purification

All the CC meteorites (except Tarda) have previously been measured for Cu and Zn isotopic compositions and were analyzed as controls. Further chemical purifications of Zn and Cu on the same sample aliquots were conducted at the Institut de Physique du Globe de Paris, using the procedure described by [50] for Zn, and by [51,52] for Cu. For Zn, samples were loaded in 1.5 mol.L<sup>-1</sup> HBr on 50  $\mu$ L of AG1-X8 (200-400 mesh) anion exchange resin in home-made PTFE columns. Matrix elements were washed by further addition of 2 mL of 1.5 mol.L<sup>-1</sup> HBr, and Zn was eluted using 2 mL of 0.5 mol.L<sup>-1</sup> HNO<sub>3</sub>. The collected samples were then evaporated to dryness. For Cu, samples were loaded in 1 mL of 7 mol.L<sup>-1</sup> HCl on home-made PTFE columns filled with 1.6 mL of AG-MP1 resin. After washing the resin with 8 mL of 7 mol.L<sup>-1</sup> HCl, the Cu was collected with 16 mL of 7 mol.L<sup>-1</sup> HCl. Both procedures were repeated twice to ensure clean Zn and Cu fraction. Procedural blank is < 0.3 ng of Zn, and 0.6 ng of Cu which is negligible relative to the amount of Zn and Cu in the sample mass analyzed for the Ryugu samples and the CCs.

### Zinc and Cu measurements

Zinc and Cu isotope compositions were determined using a Neptune Plus Multi-Collector Inductively-Coupled-Plasma Mass-Spectrometer (MC-ICP-MS) at IPGP, using sample-standard bracketing for instrumental mass bias correction as in [50] for Zn and [51,52] for Cu. Each replicate was analyzed 6–8 times for Zn and 1–5 times for Cu depending on the amount of Cu available for each sample, and the reported errors are the two standard deviations (2SD) of these repeated measurements. For the Zn measurements, the samples were analyzed in two sessions with different sample solution concentrations: one at 100 ppb of Zn and a second one at 250 ppb of Zn, with an uptake of 100  $\mu$ L.min<sup>-1</sup>. For the Cu measurements, the samples were analyzed in one session at the concentration of 30 ppb of Cu, with the same uptake. The high purity of the final Zn fraction is needed to remove isobaric and non-isobaric interferences from the signal. Interference on <sup>64</sup>Zn by

$^{64}\text{Ni}$  is corrected by measuring the intensity of the  $^{62}\text{Ni}$ , assuming natural abundances of Ni isotopes ( $^{62}\text{Ni} = 3.63\%$ ;  $^{64}\text{Ni} = 0.93\%$ ). No  $\text{N}_2$  was used during the measurements, as this results in high background on mass 68 from  $\text{ArN}_2$ . No interference on mass 68.5 from  $\text{Ba}^{2+}$  was detected during the sessions. The reference geological material BHVO-2 and the Zn standard solution IRMM 3702 measured during the first and second sessions give values consistent with the literature (e.g., [18,20]). However, during the first session, the Zn fractions were measured at 100 ppb of Zn. All the Ryugu and CC samples had similar positive  $\epsilon^{66}\text{Zn}$ , except for the first replicate of sample C0108 which had a negative value. In other words, all the samples plot below the mass-dependent equilibrium fractionation line in a  $\delta^{68}\text{Zn}$  against  $\delta^{66}\text{Zn}$  plot, whereas the C0108 replicate falls above it (Supplementary Figure 1a). This motivated our second session of measurements on replicates at higher concentrations (250 ppb of Zn) to ensure that the observed  $\epsilon^{66}\text{Zn}$  were not analytical artifacts. The second replicate of sample C0108, analyzed at 250 ppb of Zn, shows the same isotopic signature as the rest of the Ryugu sample set and plots below the mass-dependent fractionation line with a positive  $\epsilon^{66}\text{Zn}$  (Supplementary Figure 1b). In the discussion and associated figures, only the second replicate of sample C0108 is considered and represented.

## Supplementary Material

Refer to Web version on PubMed Central for supplementary material.

## Authors

Marine Paquet<sup>1,\*</sup>, Frederic Moynier<sup>1,\*</sup>, Tetsuya Yokoyama<sup>2</sup>, Wei Dai<sup>1</sup>, Yan Hu<sup>1</sup>, Yoshinari Abe<sup>3</sup>, Jérôme Aléon<sup>4</sup>, Conel M. O'D. Alexander<sup>5</sup>, Sachiko Amari<sup>6</sup>, Yuri Amelin<sup>7</sup>, Ken-ichi Bajo<sup>8</sup>, Martin Bizzarro<sup>1,9</sup>, Audrey Bouvier<sup>10</sup>, Richard W. Carlson<sup>5</sup>, Marc Chaussidon<sup>1</sup>, Byeon-Gak Choi<sup>11</sup>, Nicolas Dauphas<sup>12</sup>, Andrew M. Davis<sup>12</sup>, Tommaso Di Rocco<sup>13</sup>, Wataru Fujiya<sup>14</sup>, Ryota Fukai<sup>15</sup>, Ikshu Gautam<sup>2</sup>, Makiko K. Haba<sup>2</sup>, Yuki Hibiya<sup>16</sup>, Hiroshi Hidaka<sup>17</sup>, Hisashi Homma<sup>18</sup>, Peter Hoppe<sup>19</sup>, Gary R. Huss<sup>20</sup>, Kiyohiro Ichida<sup>21</sup>, Tsuyoshi Iizuka<sup>22</sup>, Trevor R. Ireland<sup>23</sup>, Akira Ishikawa<sup>2</sup>, Motoo Ito<sup>24</sup>, Shoichi Itoh<sup>25</sup>, Noriyuki Kawasaki<sup>8</sup>, Noriko T. Kita<sup>26</sup>, Kouki Kitajima<sup>26</sup>, Thorsten Kleine<sup>27</sup>, Shintaro Komatani<sup>21</sup>, Alexander N. Krot<sup>20</sup>, Ming-Chang Liu<sup>28</sup>, Yuki Masuda<sup>2</sup>, Kevin D. McKeegan<sup>28</sup>, Mayu Morita<sup>21</sup>, Kazuko Motomura<sup>29</sup>, Izumi Nakai<sup>29</sup>, Kazuhide Nagashima<sup>20</sup>, David Nesvorný<sup>30</sup>, Ann N. Nguyen<sup>31</sup>, Larry Nittler<sup>5</sup>, Morihiko Onose<sup>21</sup>, Andreas Pack<sup>13</sup>, Changkun Park<sup>32</sup>, Laurette Piani<sup>33</sup>, Liping Qin<sup>34</sup>, Sara S. Russell<sup>35</sup>, Naoya Sakamoto<sup>36</sup>, Maria Schönбächler<sup>37</sup>, Lauren Tafla<sup>28</sup>, Haolan Tang<sup>28</sup>, Kentaro Terada<sup>38</sup>, Yasuko Terada<sup>39</sup>, Tomohiro Usui<sup>15</sup>, Sohei Wada<sup>8</sup>, Meenakshi Wadhwa<sup>40</sup>, Richard J. Walker<sup>41</sup>, Katsuyuki Yamashita<sup>42</sup>, Qing-Zhu Yin<sup>43</sup>, Shigekazu Yoneda<sup>44</sup>, Edward D. Young<sup>28</sup>, Hiroharu Yui<sup>45</sup>, Ai-Cheng Zhang<sup>46</sup>, Tomoki Nakamura<sup>47</sup>, Hiroshi Naraoka<sup>48</sup>, Takaaki Noguchi<sup>24</sup>, Ryuji Okazaki<sup>48</sup>, Kanako Sakamoto<sup>15</sup>, Hikaru Yabuta<sup>49</sup>, Masanao Abe<sup>15</sup>, Akiko Miyazaki<sup>15</sup>, Aiko Nakato<sup>15</sup>, Masahiro Nishimura<sup>15</sup>, Tatsuaki Okada<sup>15</sup>, Toru Yada<sup>15</sup>, Kasumi Yogata<sup>15</sup>, Satoru Nakazawa<sup>15</sup>, Takanao Saiki<sup>15</sup>, Satoshi Tanaka<sup>15</sup>, Fuyuto Terui<sup>50</sup>, Yuichi Tsuda<sup>15</sup>, Sei-ichiro Watanabe<sup>17</sup>, Makoto Yoshikawa<sup>15</sup>, Shogo Tachibana<sup>51</sup>, Hisayoshi Yurimoto<sup>8</sup>



## Affiliations

<sup>1</sup>Université Paris Cité, Institut de physique du globe de Paris, CNRS; 75005 Paris, France.

<sup>2</sup>Department of Earth and Planetary Sciences, Tokyo Institute of Technology; Tokyo 152-8551, Japan.

<sup>3</sup>Graduate School of Engineering Materials Science and Engineering, Tokyo Denki University; Tokyo 120-8551, Japan.

<sup>4</sup>Institut de Minéralogie, de Physique des Matériaux et de Cosmochimie, Sorbonne Université, Museum National d'Histoire Naturelle, CNRS UMR 7590, IRD ; 75005 Paris, France.

<sup>5</sup>Earth and Planets Laboratory, Carnegie Institution for Science; Washington, DC, 20015, USA.

<sup>6</sup>McDonnell Center for the Space Sciences and Physics Department, Washington University; St. Louis, MO 63130, USA.

<sup>7</sup>Guangzhou Institute of Geochemistry, Chinese Academy of Sciences; Guangzhou, GD 510640, China.

<sup>8</sup>Natural History Sciences, IIL, Hokkaido University; Sapporo 001-0021, Japan.

<sup>9</sup>Centre for Star and Planet Formation, GLOBE Institute, University of Copenhagen; Copenhagen, K 1350, Denmark.

<sup>10</sup>Bayerisches Geoinstitut, Universität Bayreuth; Bayreuth 95447, Germany.

<sup>11</sup>Department of Earth Science Education, Seoul National University; Seoul 08826, Republic of Korea.

<sup>12</sup>Department of the Geophysical Sciences and Enrico Fermi Institute, The University of Chicago, 5734 South Ellis Avenue, , Chicago 60637, USA.

<sup>13</sup>Faculty of Geosciences and Geography, University of Göttingen; Göttingen, D-37077, Germany.

<sup>14</sup>Faculty of Science, Ibaraki University; Mito 310-8512, Japan.

<sup>15</sup>ISAS/JSEC, JAXA; Sagami-hara 252-5210, Japan.

<sup>16</sup>General Systems Studies, The University of Tokyo; Tokyo 153-0041, Japan.

<sup>17</sup>Earth and Planetary Sciences, Nagoya University; Nagoya 464-8601, Japan.

<sup>18</sup>Osaka Application Laboratory, SBUWDX, Rigaku Corporation; Osaka 569-1146, Japan

<sup>19</sup>Max Planck Institute for Chemistry; Mainz 55128, Germany.

<sup>20</sup>Hawai'i Institute of Geophysics and Planetology, University of Hawai'i at M noa; Honolulu, HI 96822, USA.

<sup>21</sup>Analytical Technology, Horiba Techno Service Co., Ltd.; Kyoto 601-8125, Japan

- <sup>22</sup>Earth and Planetary Science, The University of Tokyo; Tokyo 113-0033, Japan.
- <sup>23</sup>School of Earth and Environmental Sciences, The University of Queensland; St Lucia QLD 4072, Australia.
- <sup>24</sup>Kochi Institute for Core Sample Research, JAMSTEC; Kochi 783-8502, Japan.
- <sup>25</sup>Earth and Planetary Sciences, Kyoto University; Kyoto 606-8502, Japan.
- <sup>26</sup>Geoscience, University of Wisconsin-Madison; Madison, WI 53706, USA.
- <sup>27</sup>Max Planck Institute for Solar System Research; 37077 Göttingen, Germany.
- <sup>28</sup>Earth, Planetary, and Space Sciences, UCLA; Los Angeles, CA 90095, USA.
- <sup>29</sup>Thermal Analysis, Rigaku Corporation; Tokyo 196-8666, Japan
- <sup>30</sup>Department of Space Studies, Southwest Research Institute, Boulder, CO 80302, USA.
- <sup>31</sup>Astromaterials Research and Exploration Science, NASA Johnson Space Center; Houston, TX 77058, USA.
- <sup>32</sup>Earth-System Sciences, Korea Polar Research Institute; Incheon 21990, Korea.
- <sup>33</sup>Centre de Recherches Pétrographiques et Géochimiques, CNRS - Université de Lorraine; 54500 Nancy, France.
- <sup>34</sup>CAS Key Laboratory of Crust-Mantle Materials and Environments, University of Science and Technology of China, School of Earth and Space Sciences; Anhui 230026, China.
- <sup>35</sup>Department of Earth Sciences, Natural History Museum; London, SW7 5BD, UK.
- <sup>36</sup>IIL, Hokkaido University; Sapporo 001-0021, Japan.
- <sup>37</sup>Institute for Geochemistry and Petrology, Department of Earth Sciences, ETH Zurich, Zurich, Switzerland.
- <sup>38</sup>Earth and Space Science, Osaka University; Osaka 560-0043, Japan.
- <sup>39</sup>Spectroscopy and Imaging, Japan Synchrotron Radiation Research Institute; Hyogo 679-5198 Japan.
- <sup>40</sup>School of Earth and Space Exploration, Arizona State University; Tempe, AZ 85281, USA.
- <sup>41</sup>Geology, University of Maryland, College Park, MD 20742, USA.
- <sup>42</sup>Graduate School of Natural Science and Technology, Okayama University; Okayama 700-8530, Japan.
- <sup>43</sup>Earth and Planetary Sciences, University of California; Davis, CA 95616, USA.
- <sup>44</sup>Science and Engineering, National Museum of Nature and Science; Tsukuba 305-0005, Japan.
- <sup>45</sup>Chemistry, Tokyo University of Science; Tokyo 162-8601, Japan.

<sup>46</sup>School of Earth Sciences and Engineering, Nanjing University; Nanjing 210023, China.

<sup>47</sup>Department of Earth Science, Tohoku University; Sendai, 980-8578, Japan.

<sup>48</sup>Department of Earth and Planetary Sciences, Kyushu University; Fukuoka 819-0395, Japan.

<sup>49</sup>Earth and Planetary Systems Science Program, Hiroshima University; Higashi-Hiroshima, 739-8526, Japan.

<sup>50</sup>Kanagawa Institute of Technology; Atsugi 243-0292, Japan.

<sup>51</sup>UTokyo Organization for Planetary and Space Science, University of Tokyo; Tokyo 113-0033, Japan.

## Acknowledgements

This work was partly supported by the IGP analytical platform PARI, Region Ile-de-France SESAME Grants no. 12015908, and DIM ACAV +, the ERC grant agreement No. 101001282 (METAL) (F.M.) the UnivEarthS Labex program (numbers: ANR-10-LABX-0023 and ANR-11-IDEX-0005-02) (F.M.), JSPS Kaken-hi grants (S.T., H.Y., T.Y.) and the CNES. We thank Katarina Lodders, Herbert Palme and an anonymous reviewer for their constructive comments that helped improve the manuscript.

## Data availability

All data referred to in this article can be found in the tables or source data.

## References

1. Lodders K. Relative atomic solar system abundances, mass fractions, and atomic masses of the elements and their isotopes, composition of the solar photosphere, and compositions of the major chondritic meteorite groups. *Space Sci Rev.* 2021; 217 (3) 1–33.
2. Morota T, et al. Sample collection from asteroid (162173) Ryugu by Hayabusa2: Implications for surface evolution. *Science.* 2020; 368 (6491) 654–659. [PubMed: 32381723]
3. Tachibana S, et al. Pebbles and sand on asteroid (162173) Ryugu: in situ observation and particles returned to Earth. *Science.* 2022; 375 (6584) 1011–1016. [PubMed: 35143255]
4. Yada T, et al. Preliminary analysis of the Hayabusa2 samples returned from C-type asteroid Ryugu. *Nat Astron.* 2022; 6 (2) 214–220.
5. Yokoyama T, et al. The first returned samples from a C-type asteroid show kinship to the chemically most primitive meteorites. *Science.* 2022; doi: 10.1126/science.abn7850
6. Nakamura E, et al. On the origin and evolution of the asteroid Ryugu: A comprehensive geochemical perspective. *Proc Japan Acad, Series B.* 2022; 98 (6) 227–282. DOI: 10.2183/pjab.98.015 [PubMed: 35691845]
7. Ito M, et al. A pristine record of outer Solar System materials from asteroid Ryugu's returned sample. *Nat Astron.* 2022. 1–9.
8. Wang Z, Becker H. Ratios of S, Se and Te in the silicate Earth require a volatile-rich late veneer. *Nature.* 2013; 499 (7458) 328–331. [PubMed: 23868263]
9. Savage PS, et al. Copper isotope evidence for large-scale sulphide fractionation during Earth's differentiation. *Geochem Perspect Lett.* 2015.
10. Schönbächler M, Carlson RW, Horan MF, Mock TD, Hauri EH. Heterogeneous accretion and the moderately volatile element budget of Earth. *Science.* 2010; 328 (5980) 884–887. [PubMed: 20466929]

11. Braukmüller N, Wombacher F, Funk C, Münker C. Earth's volatile element depletion pattern inherited from a carbonaceous chondrite-like source. *Nat Geo.* 2019; 12 (7) 564–568. DOI: 10.1038/s41561-019-0375-x [PubMed: 31249609]
12. Varas-Reus MI, König S, Yierpan A, Lorand JP, Schoenberg R. Selenium isotopes as tracers of a late volatile contribution to Earth from the outer Solar System. *Nat Geo.* 2019; 12 (9) 779–782. DOI: 10.1038/s41561-019-0414-7 [PubMed: 31485262]
13. Kubik E, et al. Tracing Earth's volatile delivery with tin. *J Geophys Res: Solid Earth.* 2021; 126 (10) e2021JB022026
14. Lodders K. Solar system abundances and condensation temperatures of the elements. *ApJ.* 2003; 591 (2) 1220;
15. Day JM, Moynier F. Evaporative fractionation of volatile stable isotopes and their bearing on the origin of the Moon. *Phil Trans R S A.* 2014; 372 (2024) 20130259 doi: 10.1098/rsta.2013.0259 [PubMed: 25114311]
16. Schaefer L, Fegley B Jr. Chemistry of atmospheres formed during accretion of the Earth and other terrestrial planets. *Icarus.* 2010; 208 (1) 438–448.
17. Luck JM, Othman DB, Albarède F. Zn and Cu isotopic variations in chondrites and iron meteorites: early solar nebula reservoirs and parent-body processes. *Geochim Cosmochim Acta.* 2005; 69 (22) 5351–5363.
18. Pringle EA, Moynier F, Beck P, Paniello R, Hezel DC. The origin of volatile element depletion in early solar system material: Clues from Zn isotopes in chondrules. *Earth Planet Sci Lett.* 2017; 468: 62–71.
19. Luck JM, Othman DB, Barrat JA, Albarède F. Coupled  $^{63}\text{Cu}$  and  $^{16}\text{O}$  excesses in chondrites. *Geochim Cosmochim Acta.* 2003; 67 (1) 143–151.
20. Mahan B, Moynier F, Beck P, Pringle EA, Siebert J. A history of violence: Insights into post-accretionary heating in carbonaceous chondrites from volatile element abundances, Zn isotopes and water contents. *Geochim Cosmochim Acta.* 2018; 220: 19–35.
21. Barrat JA, Zanda B, Moynier F, Bollinger C, Liorzou C, Bayon G. Geochemistry of CI chondrites: Major and trace elements, and Cu and Zn isotopes. *Geochim Cosmochim Acta.* 2012; 83: 79–92.
22. Rosman KJR. A survey of the isotopic and elemental abundance of zinc. *Geochim Cosmochim Acta.* 1972; 36 (7) 801–819.
23. Russell WA, Papanastassiou DA, Tombrello TA. Ca isotope fractionation on the Earth and other solar system materials. *Geochim Cosmochim Acta.* 1978; 42 (8) 1075–1090.
24. Clayton RN, Mayeda TK. Oxygen isotope studies of carbonaceous chondrites. *Geochim Cosmochim Acta.* 1999; 63 (13-14) 2089–2104.
25. Hellmann JL, Hopp T, Burkhardt C, Kleine T. Origin of volatile element depletion among carbonaceous chondrites. *Earth Planet Sci Lett.* 2020; 549 116508
26. Pringle EA, Moynier F. Rubidium isotopic composition of the Earth, meteorites, and the Moon: Evidence for the origin of volatile loss during planetary accretion. *Earth Planet Sci Lett.* 2017; 473: 62–70.
27. Nie NX, et al. Imprint of chondrule formation on the K and Rb isotopic compositions of carbonaceous meteorites. *Sci Adv.* 2021; 7 (49) eabl3929 doi: 10.1126/sciadv.abl3929 [PubMed: 34851657]
28. Savage PS, Moynier F, Boyet M. Zinc isotope anomalies in primitive meteorites identify the outer solar system as an important source of Earth's volatile inventory. *Icarus.* 2022; 386 115172
29. Steller T, Burkhardt C, Yang C, Kleine T. Nucleosynthetic zinc isotope anomalies reveal a dual origin of terrestrial volatiles. *Icarus.* 2022; 386 115171
30. Trinquier A, Birck JL, Allègre CJ. Widespread  $^{54}\text{Cr}$  heterogeneity in the inner solar system. *ApJ.* 2007; 655 (2) 1179;
31. Trinquier A, Elliott T, Ulfbeck D, Coath C, Krot AN, Bizzarro M. Origin of nucleosynthetic isotope heterogeneity in the solar protoplanetary disk. *Science.* 2009; 324 (5925) 374–376. [PubMed: 19372428]
32. Warren PH. Stable-isotopic anomalies and the accretionary assemblage of the Earth and Mars: A subordinate role for carbonaceous chondrites. *Earth Planet Sci Lett.* 2011; 311 (1-2) 93–100.

33. Budde G, Burkhardt C, Brennecka GA, Fischer-Gödde M, Kruijjer TS, Kleine T. Molybdenum isotopic evidence for the origin of chondrules and a distinct genetic heritage of carbonaceous and non-carbonaceous meteorites. *Earth Planet Sci Lett.* 2016; 454: 293–303.
34. Kruijjer TS, Burkhardt C, Budde G, Kleine T. Age of Jupiter inferred from the distinct genetics and formation times of meteorites. *Proc Natl Acad Sci.* 2017; 114 (26) 6712–6716. DOI: 10.1073/pnas.1704461114 [PubMed: 28607079]
35. Burkhardt C, Dauphas N, Hans U, Bourdon B, Kleine T. Elemental and isotopic variability in solar system materials by mixing and processing of primordial disk reservoirs. *Geochim Cosmochim Acta.* 2019; 261: 145–170.
36. Nanne JA, Nimmo F, Cuzzi JN, Kleine T. Origin of the non-carbonaceous–carbonaceous meteorite dichotomy. *Earth Planet Sci Lett.* 2019; 511: 44–54.
37. Dauphas N, Chen JH, Zhang J, Papanastassiou DA, Davis AM, Travaglio C. Calcium-48 isotopic anomalies in bulk chondrites and achondrites: Evidence for a uniform isotopic reservoir in the inner protoplanetary disk. *Earth Planet Sci Lett.* 2014; 407: 96–108.
38. Chambers JE. Planetary accretion in the inner Solar System. *E Earth Planet Sci Lett.* 2004; 223 (3-4) 241–252.
39. Walsh KJ, Morbidelli A, Raymond SN, O’Brien DP, Mandell AM. A low mass for Mars from Jupiter’s early gas-driven migration. *Nature.* 2011; 475 (7355) 206–209. [PubMed: 21642961]
40. Javoy M, et al. The chemical composition of the Earth: Enstatite chondrite models. *Earth Planet Sci Lett.* 2010; 293 (3-4) 259–268.
41. Morbidelli A, Libourel G, Palme H, Jacobson SA, Rubie DC. Subsolar Al/Si and Mg/Si ratios of non-carbonaceous chondrites reveal planetesimal formation during early condensation in the protoplanetary disk. *Earth Planet Sci Lett.* 2020; 538 116220
42. Frossard P, Guo Z, Spencer M, Boyet M, Bouvier A. Evidence from achondrites for a temporal change in Nd nucleosynthetic anomalies within the first 1.5 million years of the inner solar system formation. *Earth Planet Sci Lett.* 2021; 566 116968
43. Alexander CMD. An exploration of whether Earth can be built from chondritic components, not bulk chondrites. *Geochim Cosmochim Acta.* 2022; 318: 428–451.
44. Lodders K. An oxygen isotope mixing model for the accretion and composition of rocky planets. From dust to terrestrial planets. 2000. 341–354.
45. Schiller M, Bizzarro M, Fernandes VA. Isotopic evolution of the protoplanetary disk and the building blocks of Earth and the Moon. *Nature.* 2018; 555 (7697) 507–510. DOI: 10.1038/nature25990 [PubMed: 29565359]
46. Schiller M, Bizzarro M, Siebert J. Iron isotope evidence for very rapid accretion and differentiation of the proto-Earth. *Sci Adv.* 2020; 6 (7) eaay7604 doi: 10.1126/sciadv.aay7604 [PubMed: 32095530]
47. Mezger K, Maltese A, Vollstaedt H. Accretion and differentiation of early planetary bodies as recorded in the composition of the silicate Earth. *Icarus.* 2021; 365 114497
48. Johansen A, et al. A pebble accretion model for the formation of the terrestrial planets in the Solar System. *Sci Adv.* 2021; 7 (8) eabc0444 doi: 10.1126/sciadv.abc0444 [PubMed: 33597233]
49. Sossi PA, Nebel O, O’Neill HSC, Moynier F. Zinc isotope composition of the Earth and its behaviour during planetary accretion. *Chem Geol.* 2018; 477: 73–84.
50. van Kooten E, Moynier F. Zinc isotope analyses of singularly small samples < 5 ng Zn): investigating chondrule-matrix complementarity in Leoville. *Geochim Cosmochim Acta.* 2019; 261: 248–268.
51. Moynier F, Creech J, Dallas J, Le Borgne M. Serum and brain natural copper stable isotopes in a mouse model of Alzheimer’s disease. *Sci Rep.* 2019; 9 (1) 1–7. DOI: 10.1038/s41598-019-47790-5 [PubMed: 30626917]
52. Moynier F, et al. Copper and zinc isotopic excursions in the human brain affected by Alzheimer’s disease. *Alzheimer’s Dementia: DADM.* 2020; 12 (1) e12112 doi: 10.1002/dad2.12112 [PubMed: 33102682]
53. Petitat M, Birck JL, Luu TH, Gounelle M. The chromium isotopic composition of the ungrouped carbonaceous chondrite Tagish Lake. *ApJ.* 2011; 736 (1) 23.

54. Schoenberg R, et al. The stable Cr isotopic compositions of chondrites and silicate planetary reservoirs. *Geochim Cosmochim Acta*. 2016; 183: 14–30.
55. Dey, S; Yin, QZ; Zolensky, M. Exploring the Planetary Genealogy of Tarda—A Unique New Carbonaceous Chondrite; 52nd Lunar and Planetary Science Conference; 2021 March. 2517
56. Zhu K, et al. Chromium isotopic insights into the origin of chondrite parent bodies and the early terrestrial volatile depletion. *Geochim Cosmochim Acta*. 2021; 301: 158–186. DOI: 10.1016/j.gca.2021.02.031 [PubMed: 34393262]

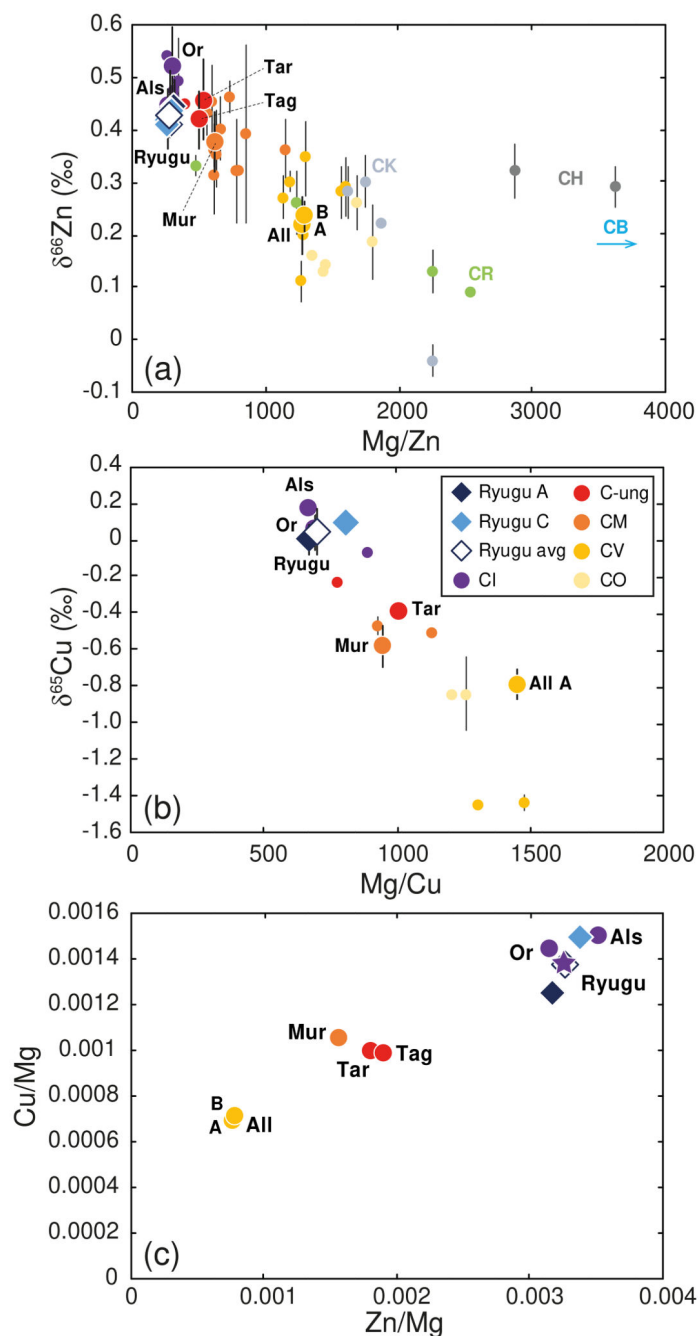


**Figure 1. Zinc and copper elemental and isotopic compositions for Ryugu and carbonaceous chondrites samples.**

(a)  $\delta^{66}\text{Zn}$  vs Mg/Zn, (b)  $\delta^{65}\text{Cu}$  vs Mg/Cu and (c) Zn/Mg vs Cu/Mg that we measured for the Ryugu samples (diamonds) and carbonaceous chondrites (large circles with abbreviations: Or=Orgueil, Als=Alais, Tag=Tagish Lake, Tar=Tarda, Mur=Murchison, All=Allende). Small circles are from the literature [17–21] for Zn and Cu isotope compositions (and references therein for major and trace element compositions). The color identifies the type of chondrite as described in the legend. The purple star in panel c represents the CI chondrite

composition from [1]. Data are presented as mean values with 2SD error bars, reported in Table 1.



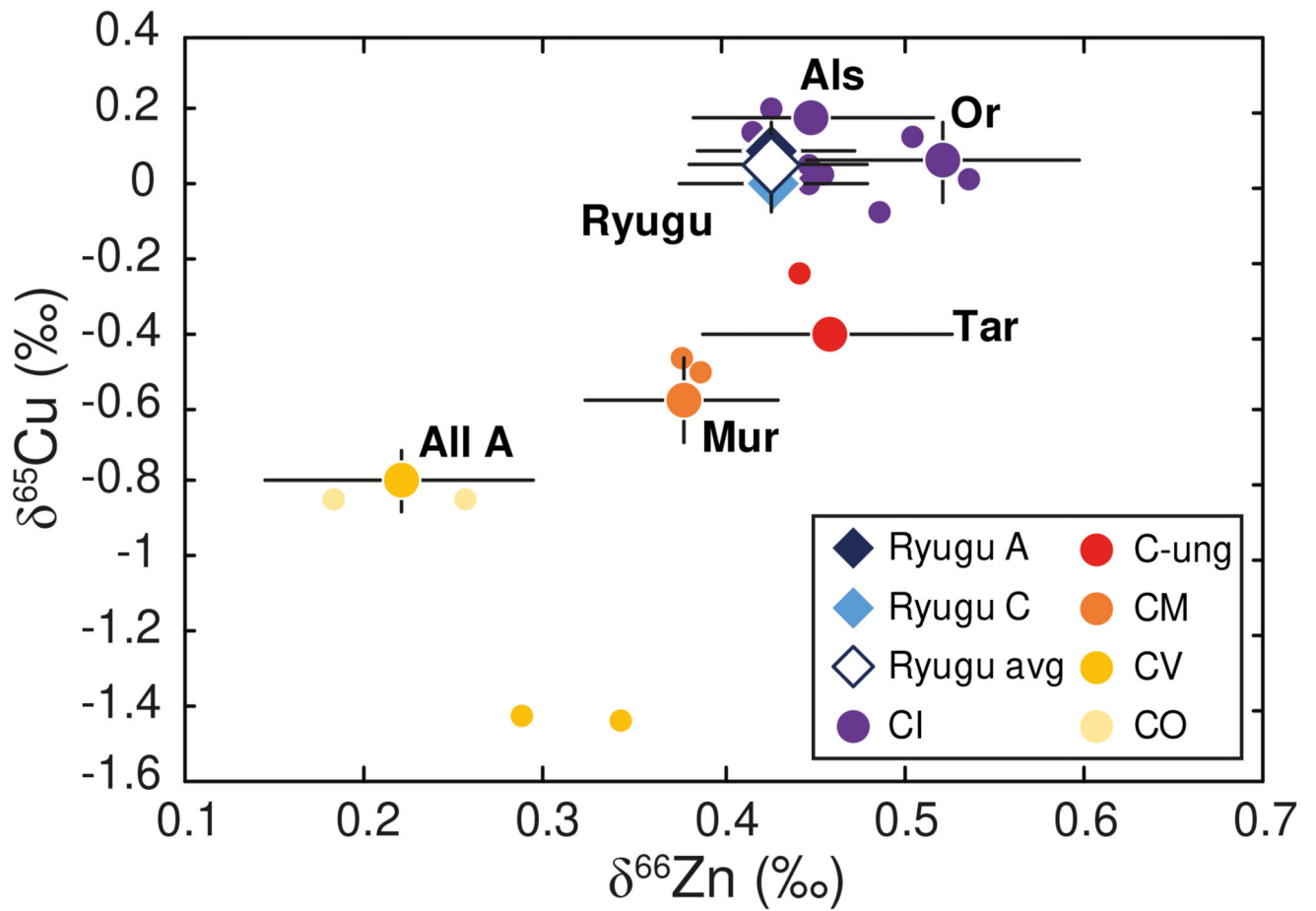


**Figure 2.  $\delta^{66}\text{Zn}$  vs  $\delta^{65}\text{Cu}$  for Ryugu samples and carbonaceous chondrites.**

Literature data are from [17,19]. Same symbols as in Figure 1 for the samples analyzed in this study. Other chondrite groups from the literature are reported directly on the figure. Data are presented as mean values with 2SD error bars, reported in Table 1. For clarity, only the error bars of our measurements are displayed. Error bars for literature data are not shown.

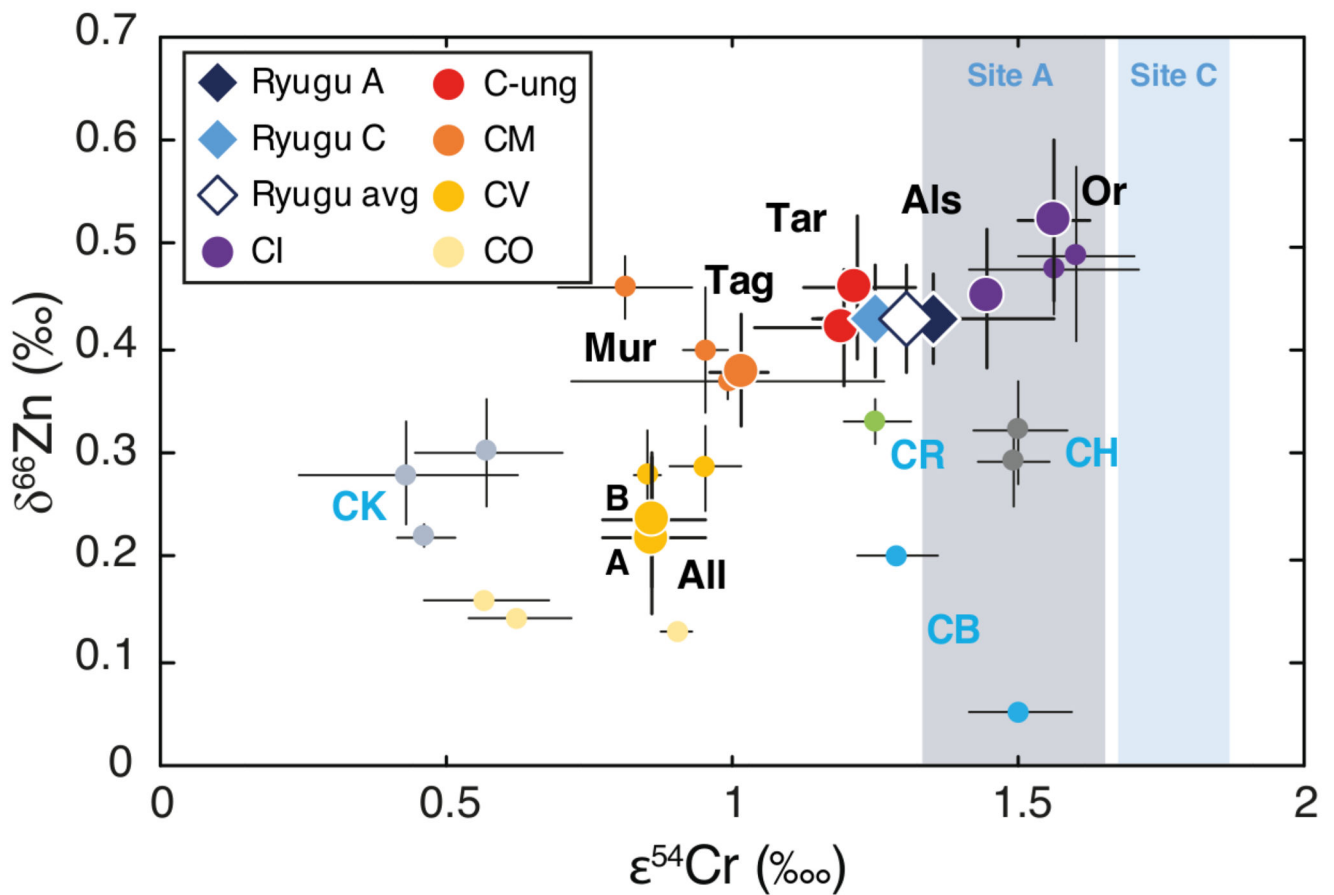


**Figure 3.**  $\delta^{66}\text{Zn}$  (this study) vs  $\epsilon^{54}\text{Cr}$  [5,30,53–55] for Ryugu samples and carbonaceous chondrites.

Literature data are from [17,18,20] for Zn isotope compositions, and from [56] for Cr isotope compositions. The dark and light blue shaded areas correspond to the  $\epsilon^{54}\text{Cr}$  ranges for site A and site C, respectively, from [6]. Same symbols as in Figure 1 for the samples analyzed in this study. Other chondrite groups from the literature are reported directly on the figure. Data are presented as mean values with 2SD error bars, reported in Table 1.

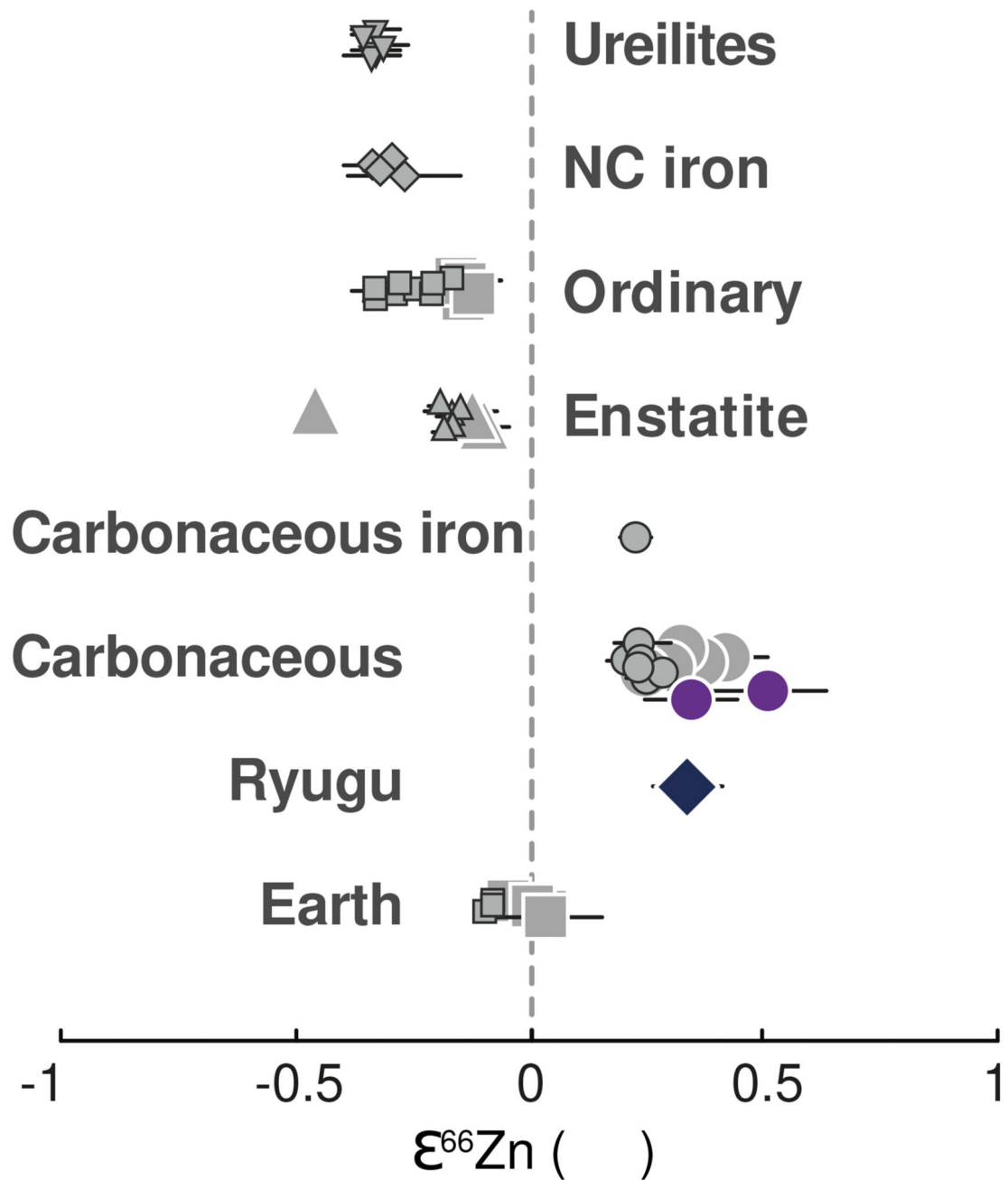


**Figure 4. Variations of  $\epsilon^{66}\text{Zn}$  among different groups of meteorites.**

For comparison purposes, only Ryugu (diamond) and CI (purple circles) samples measured in this study are represented here. Literature data for carbonaceous chondrites ([28] (large symbols), [29] (small symbols)), ordinary chondrites [28,29], enstatite chondrites [28,29], NC and CC iron chondrites [29], ureilites [29] are shown with gray symbols. Bulk Silicate Earth:  $+0.015 \pm 0.075$  ‰, 2SE,  $n = 4$  [28] and  $-0.07 \pm 0.013$  ‰, 2SE,  $n = 3$  [29]). Data are presented as mean values with 2SE error bars, reported in Table 1.

**Table 1**  
**Zinc and copper stable isotope of Ryugu samples and carbonaceous chondrites.**

Sample	Type	n <sup>a</sup> (Zn)	$\delta^{66}\text{Zn}$ (‰)	2SD <sup>b</sup>	$\delta^{67}\text{Zn}$ (‰)	2SD <sup>b</sup>	$\delta^{68}\text{Zn}$ (‰)	2SD <sup>b</sup>	$\epsilon^{66}\text{Zn}$	2SE <sup>b</sup>
<b>Ryugu</b>										
C0108 <sup>c</sup>		8	0.44	0.05	0.70	0.10	0.91	0.09	-0.21	0.17
Rpt		6	0.44	0.05	0.60	0.05	0.79	0.09	0.35	0.10
C0107		8	0.42	0.06	0.57	0.10	0.75	0.09	0.37	0.11
Rpt		6	0.41	0.05	0.60	0.10	0.76	0.13	0.29	0.11
<i>Average site C</i>		20	0.43	0.05	0.62	0.13	0.81	0.17	0.34	0.06
A0106-A107		8	0.45	0.02	0.62	0.06	0.80	0.05	0.42	0.10
Rpt		6	0.41	0.06	0.59	0.08	0.75	0.11	0.33	0.03
A0106		8	0.43	0.03	0.63	0.07	0.80	0.06	0.25	0.14
Rpt		6	0.41	0.06	0.58	0.07	0.76	0.11	0.31	0.05
<i>Average site A</i>		28	0.43	0.04	0.61	0.08	0.78	0.08	0.33	0.05
<i>Average Ryugu</i>		48	0.43	0.05	0.61	0.11	0.79	0.14	0.33	0.04
<b>Carbonaceous chondrites</b>										
Orgueil	CI1	8	0.52	0.06	0.67	0.11	0.91	0.06	0.62	0.15
Rpt		8	0.52	0.09	0.71	0.09	0.96	0.17	0.33	0.14
<i>Average Orgueil</i>		16	0.52	0.08	0.69	0.11	0.94	0.14	0.52	0.12
Alais	CI1	8	0.45	0.07	0.62	0.11	0.82	0.08	0.35	0.19
Rpt		6	0.44	0.07	0.62	0.10	0.80	0.12	0.35	0.09
<i>Average Alais</i>		14	0.45	0.07	0.62	0.10	0.80	0.10	0.35	0.11
Tagish Lake	C2-ung	8	0.43	0.02	0.55	0.12	0.74	0.06	0.53	0.08
Rpt		6	0.41	0.08	0.54	0.08	0.73	0.15	0.41	0.07
<i>Average Tagish Lake</i>	14	0.42	0.06	0.55	0.10	0.73	0.11	0.48	0.06	
Tarda	C2-ung	8	0.46	0.06	0.58	0.09	0.80	0.06	0.50	0.12
Rpt		6	0.46	0.09	0.64	0.14	0.83	0.15	0.41	0.08
<i>Average Tarda</i>		14	0.46	0.07	0.60	0.13	0.81	0.11	0.46	0.08
Murchison	CM2	8	0.38	0.03	0.52	0.09	0.70	0.06	0.25	0.13
Rpt		6	0.37	0.08	0.52	0.09	0.67	0.15	0.35	0.16
<i>Average Murchison</i>		14	0.38	0.05	0.52	0.09	0.69	0.10	0.29	0.10
Allende A	CV3	5	0.21	0.03	0.26	0.09	0.37	0.08	0.28	0.17
Rpt		6	0.22	0.10	0.28	0.16	0.35	0.20	0.47	0.15
<i>Average Allende A</i>		11	0.22	0.07	0.27	0.13	0.36	0.15	0.38	0.12
Allende B	CV3	8	0.24	0.07	0.30	0.14	0.43	0.09	0.23	0.12
Rpt		6	0.23	0.06	0.31	0.12	0.38	0.18	0.32	0.13
<i>Average Allende B</i>		14	0.24	0.06	0.31	0.13	0.41	0.14	0.27	0.09
<b>Reference materials</b>										
IRMM3702		7	0.22	0.04	0.26	0.05	0.43	0.06	0.02	0.11

Sample	Type	$n^a$ (Zn)	$\delta^{66}\text{Zn}$ (‰)	$2\text{SD}^b$	$\delta^{67}\text{Zn}$ (‰)	$2\text{SD}^b$	$\delta^{68}\text{Zn}$ (‰)	$2\text{SD}^b$	$\epsilon^{66}\text{Zn}$	$2\text{SE}^b$
BHVO2		12	0.30	0.07	0.46	0.08	0.58	0.10	-0.07	0.15

<sup>a</sup> n is the number of measurements

<sup>b</sup> 2SD is 2 x standard deviation; 2SE is 2 x standard error

<sup>c</sup> Value excluded from the averages for Ryugu

Numbers in italic represent averages for Ryugu and the carbonaceous chondrites for the Zn data

**Table 2**  
**Major and trace element compositions of Ryugu samples and carbonaceous chondrites.**

Sample	Type	Zn (ppm)	2SD	Cu (ppm)	2SD	Mg (ppm)	2SD	Mg/Zn
<b>Ryugu</b>								
C0108*		352	4	156	2	104222	1153	296
C0107		383	6	168	1	98823	2890	258
<i>Average site C</i>		<i>368</i>	<i>45</i>	<i>162</i>	<i>17</i>	<i>101523</i>	<i>7635</i>	<i>277</i>
A0106-A107*		338	4	133	2	106866	1250	316
A0106		369	5	130	2	112899	3191	306
<i>Average site A</i>		<i>354</i>	<i>45</i>	<i>132</i>	<i>5</i>	<i>109883</i>	<i>8533</i>	<i>311</i>
<i>Average Ryugu</i>		<i>361</i>	<i>40</i>	<i>147</i>	<i>37</i>	<i>101509</i>	<i>11700</i>	<i>294</i>
<b>Carbonaceous chondrites</b>								
Orgueil	CI1	288	4	131	1	91158	2706	3.0
Alais	CI1	298	3	127	1	84683	2489	2.9
Tagish Lake	C2-ung	204	5	105	3	107210	1275	1.2
Tarda	C2-ung	201	3	110	2	111296	2388	2.1
Murchison	CM2	174	2	117	1	111130	1257	1.1
Allende A	CV3	110	2	97	2	141784	2461	1.7
Allende B	CV3	121	1	105	1	157609	4882	3.1

\* Abundances from [5]

*Numbers in italic represent averages for Ryugu, and each of Ryugu sample site*